

## Supplementary Materials for

### Spider dragline silk as torsional actuator driven by humidity

Dabiao Liu\*, Anna Tarakanova, Claire C. Hsu, Miao Yu, Shimin Zheng, Longteng Yu, Jie Liu, Yuming He,  
D. J. Dunstan, Markus J. Buehler\*

\*Corresponding author. Email: dbliu@hust.edu.cn (D.L.); mbuehler@mit.edu (M.J.B.)

Published 1 March 2019, *Sci. Adv.* **5**, eaau9183 (2019)  
DOI: 10.1126/sciadv.aau9183

#### This PDF file includes:

- Fig. S1. SEM images of the *N. pilipes* spider dragline silk before and after testing.
- Fig. S2. Twist of the *N. pilipes* spider dragline silk with increasing RH from 40 to 100%.
- Fig. S3. Twist of the *N. pilipes* spider dragline silk to RH cyclically changing from ~40 to ~100%.
- Fig. S4. Raman spectrum of the *N. pilipes* spider dragline silk.
- Fig. S5. Raman spectrum of the virgin dragline silk of *N. edulis* spider.
- Fig. S6. Raman spectrum of the virgin dragline silk of *A. versicolor* spider.
- Fig. S7. Flow chart for the molecular dynamics simulation and the determination of molecular twist.
- Fig. S8. Approach to estimating molecular twist.
- Fig. S9. Angle displacement between residue 0 and residue 1 to 70 for MaSp2 protein.
- Fig. S10. Angle displacement between residue 0 and residue 1 to 70 for MaSp1 protein.
- Table S1. Raman band assignment for the *N. pilipes*, *N. edulis*, and *A. versicolor* dragline silks.
- Note S1. Supplementary method for the spider silk harvesting.

## SEM images of samples

The morphology of the dragline silks *N. pilipes* spider before and after testing was measured by a scanning electron microscopy (Quanta 3D Dual Beam system FIB-SEM), as shown in fig.S 1. One can see that the surface of the dragline silk sample after testing is much rougher than that of virgin dragline silk.

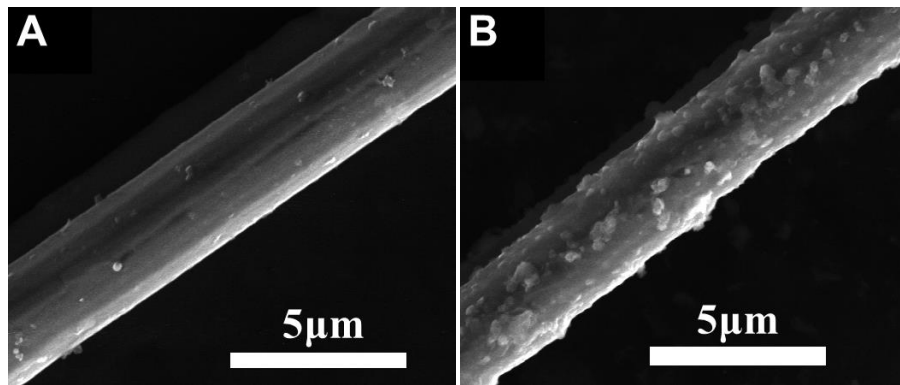


**Fig. S1. SEM images of the *N. pilipes* spider dragline silk before and after testing.**  
(A) Virgin dragline silk; (B) Dragline silk after testing.

## Supplementary data for the *N. pilipes* spider dragline silk

We provide more experimental data on dragline silk of *N. pilipes* spider. Fig. S2 shows the humidity-induced twist response under the condition that the RH is increased in a stepwise manner and then maintained at a high-level (>85%) for more than 4000s. One can see that when the RH arrived about 72%, an instant torsional deformation in dragline silk is triggered. At the end of the test, the dragline silk reached a twist deformation of about 350deg/mm to only one direction. This magnitude is much larger than that generated by dragline silk from another *N. pilipes* spider (255 deg/mm, see Fig. 3A). An extension of the sample about 1.5% after the test is observed, which is attributed to the tension from the paddle.

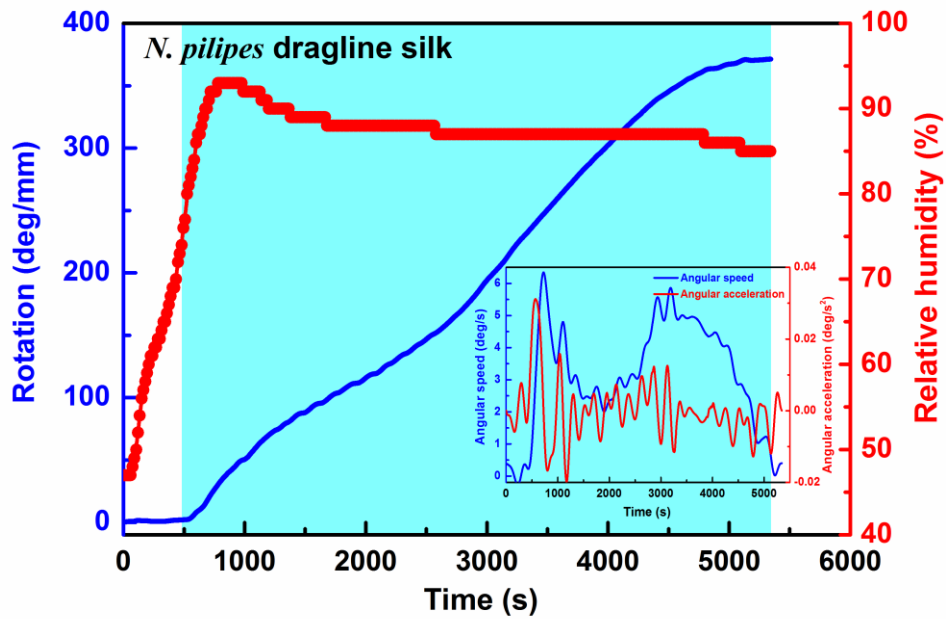


**Fig. S2.** Twist of the *N. pilipes* spider dragline silk with increasing RH from 40 to 100%. The initial sample length is 45.50mm. The length of sample after testing is 46.00 mm. The moment of inertia of the paddle is about  $0.49 \times 10^{-9} \text{ kg} \cdot \text{m}^2$ .

A new set of data for the response of dragline silk of *N. pilipes* spider to cyclical changes in RH is shown in fig. S3. When the threshold level ( $\sim 70\%$  RH) was reached, the twist of dragline silks was triggered immediately; and when the RH was below the threshold level, a slight recoverable twist was indicated, and then the silk remained still (See fig. S3A). After five cycles of RH changes, the overall generated rotation is about 325 deg/mm. The angular speed and the angular acceleration of the torsional actuation are given in fig. S3B.

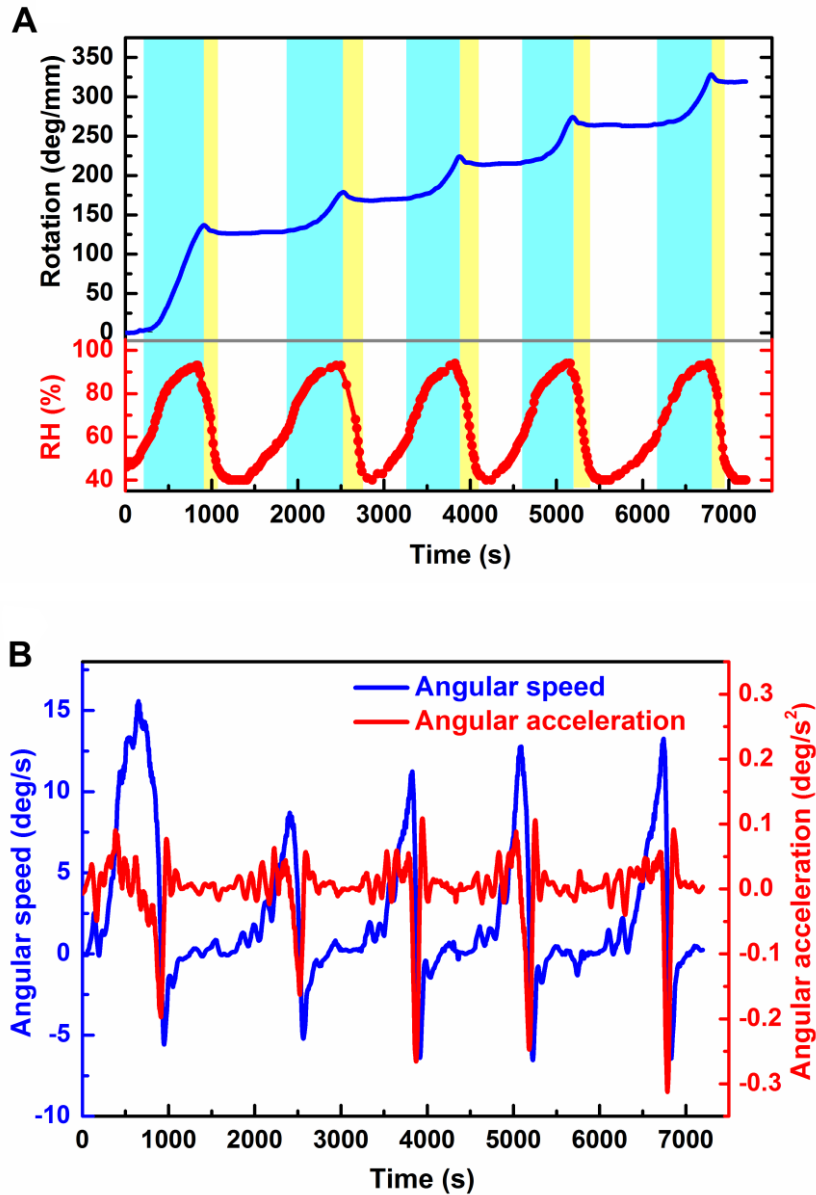


**Fig. S3. Twist of the *N. pilipes* spider dragline silk to RH cyclically changing from  $\sim 40$  to  $\sim 100\%$ .** (A) Torsional actuation of dragline silk with cyclical humidity. (B) The rotation speed and the acceleration of the paddle attached to the dragline silk. The blue shade indicates the forward twist; the yellow blue shade indicates the reverse twist. The initial length of the sample is about 50mm. After testing, the extension of the sample is about 5.8%. The moment of inertia of the paddle is about  $0.46 \times 10^{-9} \text{ kg} \cdot \text{m}^2$ .

## Raman spectrum of dragline silks

The Raman spectra of the dragline silk from *N. pilipes* (fig. S4), *N. edulis* (fig. S5) and *A. versicolor* (fig. S6) were acquired using a Raman spectrometer (LabRAM HR800, Horiba JobinYvon) having a resolution of  $1\text{cm}^{-1}$ . Sections of tested silks were glued on to the viewing frame. A Nd-YAG laser at 532 nm wavelength was focused with 100 $\times$ Leica objective on the surface of dragline silk. Raman spectra in the range of  $800\text{-}1800\text{cm}^{-1}$  were obtained from monofilaments of dragline silks using the same type of specimens as described above. For the measurements, we kept the direction of polarization of the laser radiation perpendicular to the long axes of the silk fibres.

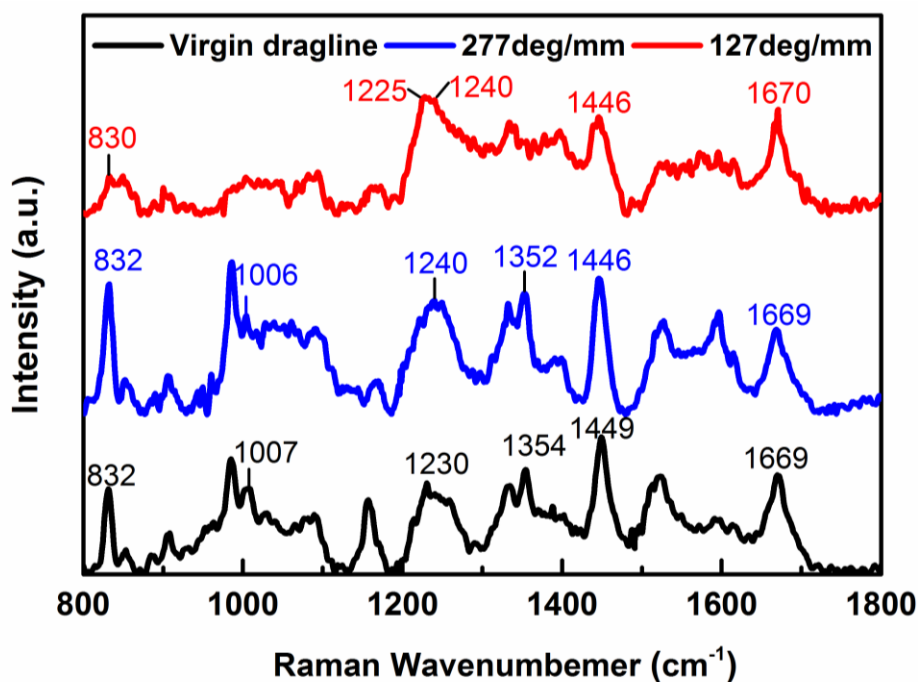


**Fig. S4. Raman spectrum of the *N. pilipes* spider dragline silk.** The blue line and red line denote the results after testing.

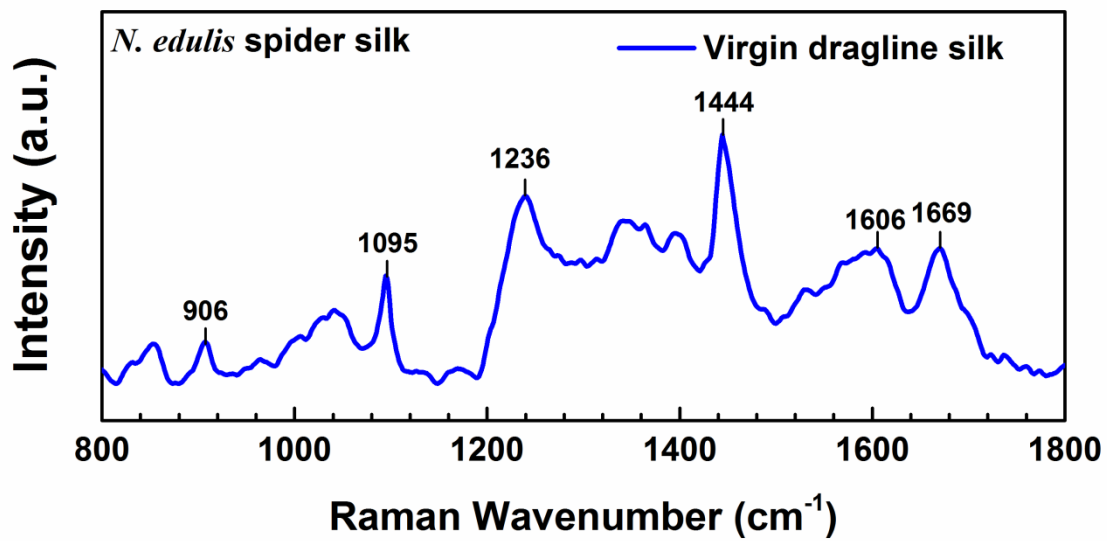


Fig. S5. Raman spectrum of the virgin dragline silk of *N. edulis* spider.

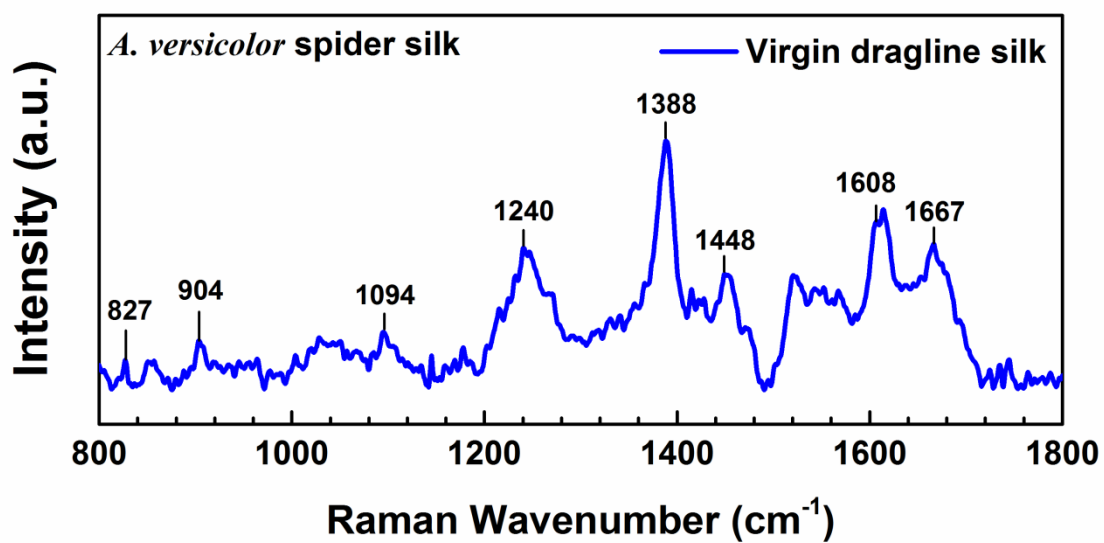
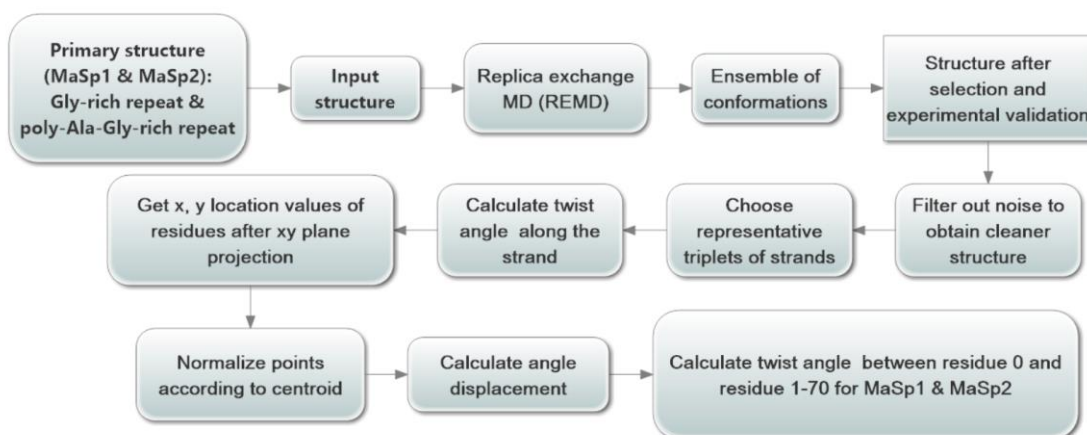


Fig. S6. Raman spectrum of the virgin dragline silk of *A. versicolor* spider.

**Table S1. Raman band assignment for the *N. pilipes*, *N. edulis*, and *A. versicolor* dragline silks.**

Raman band			Assignment
<i>N. Pilipes</i>	<i>N. edulis</i>	<i>A. versicolor</i>	
832	---	827	Tyrosine
902	906	904	C-CH <sub>3</sub> stretch
---	1095	1094	C-N stretch
1230	1236	1240	Amide III
1354	---	1388	CH <sub>3</sub> -H bend, C-H bend
1449	1444	1448	CH <sub>2</sub> bend, CH <sub>3</sub> anti-symmetric bend
---	1606	1608	Phenylalanine
1669	1669	1667	Amide I

## Molecular simulation and method for determining the molecular twist



**Fig. S7.** Flow chart for the molecular dynamics simulation and the determination of molecular twist.

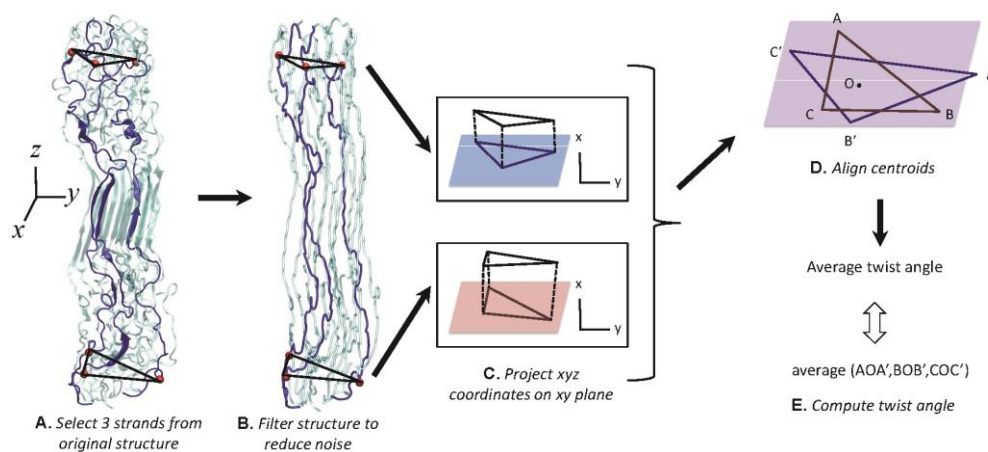


**Fig. S8.** Approach to estimating molecular twist. (A) Several triplets of strands representative of protein curvature were selected to calculate twist, based on the fifteen-stranded silk molecular model. (B) Three-way moving average was used to filter out noise in the structure. Amino acid coordinates at the same position on each strand were selected, forming triangles. (C) Coordinates of alpha carbons in selected amino acids were projected onto the xy plane. (D) Centroids of triangles were aligned. (E) Twist angle was averaged from three angle displacements.



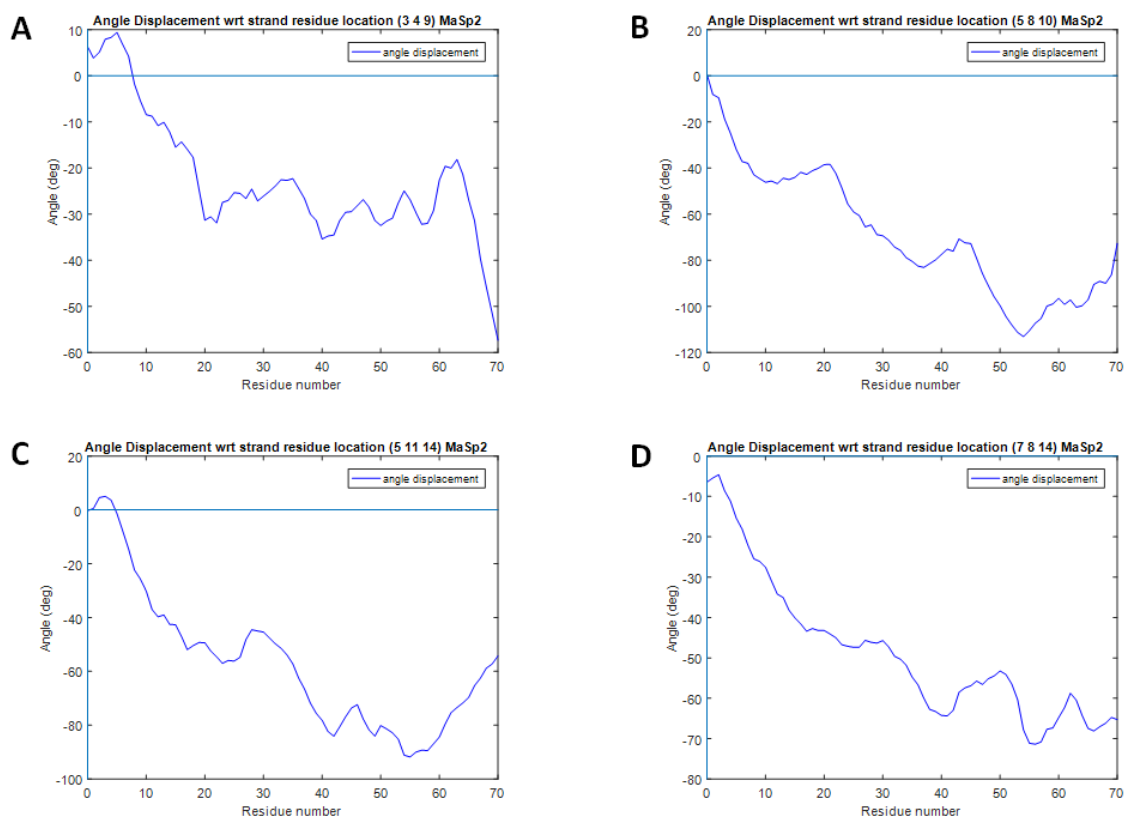


**Fig. S9. Angle displacement between residue 0 and residue 1 to 70 for MaSp2 protein.** (A) Strand residue location (3 4 9). (B) Strand residue location (5 8 10). (C) Strand residue location (5 11 14). (D) Strand residue location (7 8 14). It is shown that MaSp2 angle displacements are consistently negative traveling down the strand, suggests clockwise twist observed from the top of the structure.

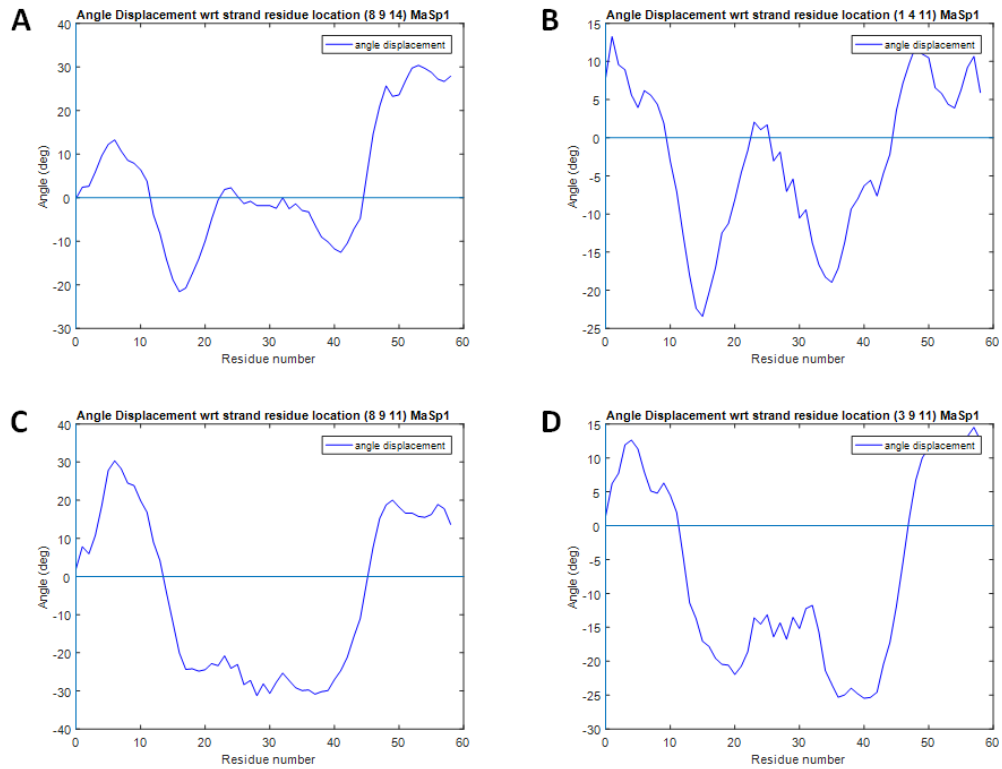


**Fig. S10. Angle displacement between residue 0 and residue 1 to 70 for MaSp1 protein.** (A) Strand residue location (8 9 14). (B) Strand residue location (1 4 11). (C) Strand residue location (8 9 11). (D) Strand residue location (3 9 11). There is an up-down-up trend in the angle displacement of MaSp1, as suggested with the two end peaks and a minor peak in the middle. The Angle magnitudes are lower than that for MaSp2 by 2-3 times.

## **Note S1. Supplementary method for the spider silk harvesting.**

The specifically designed apparatus for spider silk harvesting has been introduced in detail in our previous study. A selected adult female *N. pilipes* spider was firstly anaesthetized with CO<sub>2</sub> and then immobilized onto a soft platform by pinning around her limbs and abdomen without causing any harm. We waited at least 20 min to minimize residual effects of the anesthesia. After the spider woke up, silk was pulled by a tweezer from the spinnerets and attached to the spool with a dab of glue. Then the

stepper-motor was started to begin silk harvesting. During forcible silking, the spider was monitored under an optical microscope (KEYENCE, VHX-500F) to ensure that only the major ampullate silk (the dragline silk) was collected. The double-thread dragline silks were reeled at a controlled speed 3.8 mm/s onto a bobbin under lab conditions. Segments of silks were then transferred from the spool to sample-holders. The double-thread dragline silk was firstly separated into two individual threads at its end using an acupuncture needle under the microscope, and then was further isolated to required lengths. After harvesting, the spider would be released back to its web to feed for reeling again. This technique was used for two *N. pilipes* spiders.

In order to avoid the influence of anaesthetization on the experimental results, we adopted a new immobilization technique that did not require anesthetizing the spider at any step of the process. The spider was firstly placed on a sponge block directly without any anaesthetization. Her limbs and abdomen were fixed with pins to the block surface, immobilizing her in place without causing any harm. Dragline silk was pulled by a tweezer from the spinnerets and attached to the mandrel of the silking device using adhesive paper. The improved device consists of high-density polyethylene mandrel that rotates and moves so that silk can be wound onto it. A constant reeling speed of 11mm/s was used in the new silking procedure. The dragline silks were retrieved and stored under room conditions (around 20°C and 55% RH) and were tested within one month of collection. This new-developed technique has been used for five *N. pilipes* spiders and two *Argiope versicolor* spiders.